# **Bi-Level Optimization Framework for Heavy-Duty Electric Truck Charging Station Design**

Derek Jackson School of Electrical Engineering and Computer Science Oregon State University Corvallis, Oregon, USA jacksder@oregonstate.edu Yue Cao School of Electrical Engineering and Computer Science Oregon State University Corvallis, Oregon, USA yue.cao@oregonstate.edu Ian Beil Grid Edge Solutions Portland General Electric Portland, Oregon, USA ian.beil@pgn.com

Abstract - Heavy-duty commercial electric vehicle (HDEV) charging stations, such as for freight trucks, must handle large peak power demands. Installing on-site energy storage can reduce the peak charging demand to avoid expensive and oversized utilitymanaged distribution equipment. To ensure optimal design of charging infrastructure, the trade-off between energy storage size and grid equipment ratings should be considered. This paper presents a bi-level multi-objective optimization framework to discover Pareto optimal designs, under the constraint of optimally sized power electronic converters and realistic power loss models. Under these considerations, the bi-level approach can greatly simplify the design process by breaking up charging station optimization into a system-level problem and multiple converterlevel problems. Using industry-based HDEV arrival times and charging conditions, this bi-level approach is demonstrated for a 9port charging station. The resulting Pareto front showcases equipment sizing trade-offs that are necessary for informed charging infrastructure development decisions. The bi-level optimization Pareto front is compared the Pareto fronts of traditional, fixed efficiency converter models.

**Keywords** – Electric Vehicles, Trucks, Charging Stations, Bi-level Optimization, Multi-Objective Optimization, DC Microgrid

# I. INTRODUCTION

The transition to heavy-duty commercial electric vehicles (HDEV), such as Class 8 "18-wheeler" trucks, in the near future requires major infrastructure development to ensure charging demands are met. With battery sizes larger than 400 kWh, a single HDEV will require charging rates of 400 kW to 1 MW+[1]. For a multi-port charging station, the peak load can reach well into the MW range. These large peak ratings may result in expensive and oversized utility-managed distribution equipment. An increasingly common solution to reduce grid infrastructure investments is to offset the peak demands with an on-site energy storage system (ESS), where the ESS is recharged at times of low demand and discharged during high demand. It is therefore beneficial to consider the trade-off between ESS size and grid equipment ratings in the design of an HDEV charging station (HDEVCS).

Energy storage sizing for light-duty electric vehicle charging stations has been researched extensively in the literature (see [2]-[7] for a few examples with varying objectives), but there is a relative paucity of research focused on HDEVCS design. Charging station topologies are expected to be similar for light- and heavy-duty vehicles; on-site energy storage and connection to a utility-managed grid require power electronic converters to supply the charging power, regardless of a DC or AC architecture [10],[11]. However, their charging

loads are very different. An HDEV requires much larger charging power and their arrival times tend to be densely clustered within a few periods per day [1], resulting in a large peak power demand and long periods of infrequent charging. This increases the challenge of peak power shaving, where a larger on-site energy storage is needed to achieve a comparable peak power demand of a light-duty electric vehicle charging station.

Another consideration where the existing literature neglects for ESS sizing is power converter losses. While [5]-[7] do account for some losses, only fixed or near-ideal efficiencies are assumed. In an actual system, power converter efficiency is not constant and operates with varying efficiencies dependent on the load. Additionally, power losses are more apparent when managing the high power levels of an HDEVCS, where semiconductor device ratings and thermal management become limiting factors to converter operation.

Considering realistic power losses requires detailed modeling of the power electronics, and the extra details significantly slow down the model-based simulation design process. For a system level study where converter design or performance details may be unknown at the time, abstracting to a near-ideal charging station can greatly simplify the ESS sizing procedure. However, this abstraction leads to the loss of important design considerations in addition to inaccurate power losses, such as optimizing the nominal DC bus voltage and ESS voltage/current ratings. Ignoring these system design considerations through idealized operation can result in potentially undersized ESS or grid equipment.

In this paper, a bi-level multi-objective optimization framework is presented for HDEVCS design that

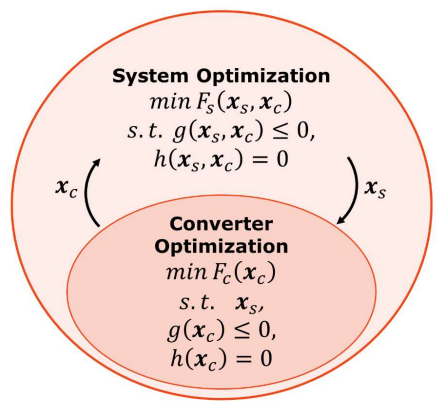


Fig. 1. Bi-level optimization interface between system-level (upper) and converter-level (lower) problems.

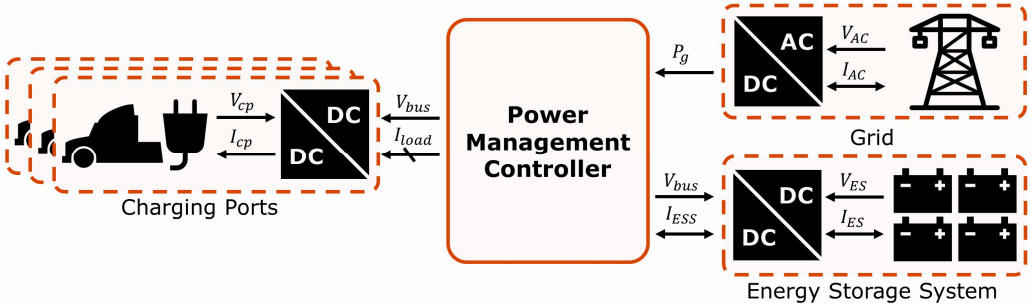


Fig. 2. High-level diagram of heavy-duty electric vehicle charging station DC microgrid.

accommodates power conversion losses and additional station design parameters. The optimization framework results in Pareto optimal HDEVCS designs, capturing the trade-off between ESS sizing and peak grid-side support under the assumption of optimally sized power converters. A bi-level hierarchy breaks down design into upper and lower levels with simpler optimization problems, where the upper-level decisions act as fixed system parameters for the lower-level [8], and the lower-level converter optimal design then serves as a constraint to the upper level (see Fig. 1). The bi-level hierarchy allows detailed power electronic design decisions to stay at the lowerlevel, without adding significant complexity to the upper-level. By optimizing each power converter at the lower-level, the upper-level optimization can focus on the design decisions of the charging station as a whole. An overview of the HDEVCS and models is first given in Section II. Then Section III presents the bi-level optimization framework setup, objectives, and constraints. Demonstration and discussion of charging station optimization, including a comparison to simulations using fixed efficiency power converters, are presented in Section IV. Section V provides a conclusion and future research considerations.

## II. CHARGING STATION MODEL DEVELOPMENT

The charging station architecture designed in this paper can be considered as a DC microgrid with a single connection to the main grid, on-site ESS, and multiple charging ports connected to a common voltage bus. A high-level diagram of the charging station is shown in Fig. 2. Note that, while included in Fig. 2, the grid-connected AC/DC converter is not explicitly modeled in this analysis, as the focus is within the DC microgrid.

Simulation of the station begins with the HDEV charging demands. A power management controller determines how much power is supplied from both the ESS and the grid, ensuring the rated power of each converter is not exceeded. The power flow from the ESS to the HDEV goes through two DC/DC converters, and their power losses are accounted for.

It should be noted that the bi-level optimization framework is not dependent on the specific models presented in this section although the models are required to demonstrate the optimization. The framework can be used with varying model types, charging profiles, arrival data, and controls.

# A. HDEV Arrival and Charging Model

The arrival time and initial state-of-charge (SOC) of the HDEVs are modeled as random processes using probability distributions presented in [1], which is derived from real-world

heavy-duty vehicle telemetry data. A Poisson random process with a time-varying mean arrival rate determines when each HDEV arrives. The initial SOC of each HDEV is generated from a beta distribution with shape parameters  $\alpha=1.1$  and  $\beta=3.2$ , fitted between 5% SOC and 100% SOC. The charging voltage and current load profile is generated using a parametric battery model [9], starting with a typical constant current rate and limited to a maximum charging voltage and power (CCCV charging). Five Monte Carlo samples were generated from these distributions, where the normalized HDEV arrival times and initial SOC distributions are shown in Fig. 3. Each Monte Carlo charging load profile is used for optimization.

#### B. Power Management Controller

The power management controller's two functions are to average out the load power delivered by the grid while also mediating the ESS SOC. The controller diagram is provided in Fig. 4. The grid's entire load consists of an averaged HDEV charging power  $P_{load(g)}$ , ESS SOC correction power  $P_{SOC}$ , and bias constant power  $P_{bias}$ .

First, adjusting the length  $T_w$  of a moving time-window average controls how aggressive the averaging is and is a design variable. Averaging the total load power  $P_{load}$  over a specified period  $T_w$  acts as a low-pass filter, reducing the power variation and peaks handled by the grid. Then the ESS SOC correction regulates the charging power of the ESS, where a lower SOC

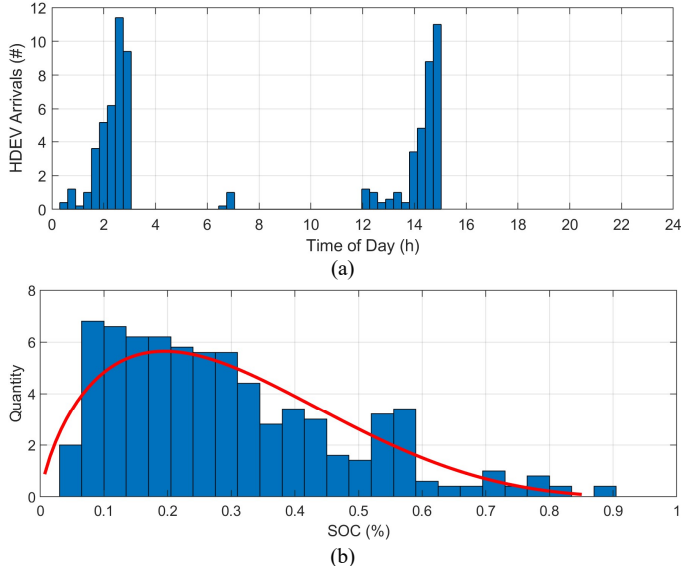


Fig. 3. (a) HDEV arrival times and (b) initial SOC normalized from five Monte Carlo samples generated from the probability distributions.

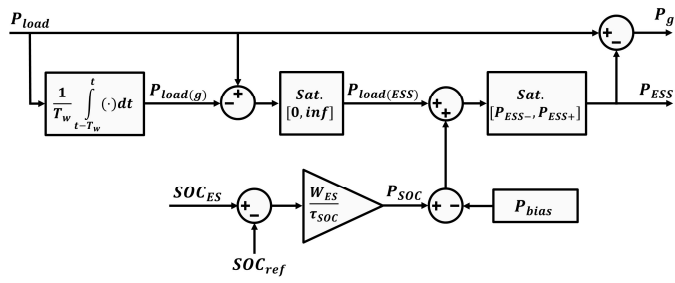


Fig. 4. Power management controller diagram.

correlates to a larger charging power. The intensity of the SOC correction is dependent on the total stored energy in the ESS  $W_{ES}$  and a correction factor time constant  $\tau_{SOC}$ . The time constant is chosen to prevent the ESS SOC from exceeding the max SOC while no HDEVs are charging (i.e., when  $P_{load}=0$ ). The last component of the grid's load power controller is a bias constant  $P_{bias}$ . Design of the station assumes the expected number of HDEV's per day is known, and therefore the expected total energy.  $P_{bias}$  is set so that the expected total energy is delivered throughout an entire day. For the Monte Carlo samples generated from the distributions in Section II-A, the actual total load energy will vary from the expected value.

Two saturation blocks are included within the power management controller. The first prevents  $P_{load(ESS)}$  from dropping below zero, which otherwise would induce additional loading on the grid. The other saturation block constrains  $P_{ESS}$  to be within the ratings of the ESS DC/DC converter.

#### C. Energy Storage Model

A Li-ion battery pack serves as the on-site energy storage. The same battery model as the HDEV charging model is used [9], where the electrochemical dynamics of the battery is modeled through RC parallel networks. The battery pack consists of battery modules in series  $N_s$ , and each module contains Li-ion cells in parallel  $N_p$ . The battery pack voltage can be adjusted by varying  $N_s$  while the total energy stored is the product of  $N_s$ ,  $N_p$ , and the cell capacity.

## D. DC/DC Converter Model

Dual active bridge (DAB) DC/DC converters are used for all power conversion stages in the charging station. DAB converters are often used in DC microgrids as they provide galvanic isolation, high efficiency under heavy loads, and high power density [10]. A steady-state power loss model is developed based on [12]-[14]. DAB conduction losses are calculated using (1), where  $I_{L(rms)}$  is the rms current through the transformer leakage inductor,  $R_L$  is the transformer resistance, and  $n_t$  is the transformer windings secondary to primary ratio.  $R_{p(on)}$  and  $R_{s(on)}$  are the SiC MOSFET drain-source onresistances of the primary and secondary H-bridges. The inductor rms current is calculated using (2), where the peak inductor currents  $I_1$  and  $I_2$  are found with (3) and (4),  $f_{sw}$  is the converter switching frequency, and d is the duty ratio representing the phase shift between the primary and secondary waveforms [14]. Note that  $I_{L(rms)}$  is the leakage inductance current referred to the secondary side and is why  $R_{p(on)}$  is scaled by  $n_t$  in (1).

$$P_{loss} = I_{L(rms)}^{2} \cdot \left[ R_{L} + \frac{1}{\sqrt{2}} \left( 4n_{t}^{2} R_{p(on)} + 4R_{s(on)} \right) \right]$$
 (1)

$$I_{L(rms)} = \frac{1}{\sqrt{3}} \sqrt{dI_1^2 + (1-d)(I_1^2 + I_1I_2 + I_2^2)}$$
 (2)

$$I_1 = \frac{1}{f_{sw}L_t} \left( V_{in} + \frac{V_o}{n_t} (2d - 1) \right)$$
 (3)

$$I_2 = \frac{1}{f_{Sw}L_t} \left( \frac{V_o}{n_t} + V_{in}(2d - 1) \right) \tag{4}$$

The high efficiency operation of a DAB converter is largely attributed to their zero-voltage switching (ZVS) capabilities that cause switching losses to be negligible under certain load conditions. To achieve ZVS conditions, the phase shift d between the primary and secondary waveforms is constrained by (5) and (6), respectively [14]. Where  $C_{p(oss)}$  and  $C_{s(oss)}$  are the output capacitances of the primary and secondary switches, and  $M = V_o/n_tV_{in}$ . These ZVS conditions act as constraints to the DAB design optimization and therefore switching losses are assumed to be zero. The large power ratings required by converters in a HDEVCS can be realized by combining multiple DAB converters in parallel, denoted by  $N_{DAB}$ . The power demand of the DAB is then divided equally among the  $N_{DAB}$  converters.

$$d \ge \frac{M-1}{2M} + \frac{2f_{SW}\sqrt{L_tC_{p(oss)}}}{M} \tag{5}$$

$$d \ge \frac{1-M}{2} + 2f_{sw}Mn_t\sqrt{L_tC_{s(oss)}} \tag{6}$$

## III. BI-LEVEL OPTIMIZATION FRAMEWORK

Finding Pareto optimal designs under power converter constraints is broken into an upper or system-level problem, and multiple lower or converter-level problems. The nested bi-level method is applied [8], where converter-level optimization is completed for every system-level design candidate. Prior to evaluating a system-level design, the design variables are sent to the converter-level and serve as design specifications that the converters are optimized for. Once the optimal converter designs are found, the converter parameters are shared with the system-level where the entire charging station is simulated (see Fig. 1). This process repeats for every design candidate picked by the system-level during optimization.

In a bi-level framework, it is possible that a certain set of upper-level design variables results in an infeasible lower-level design. To circumvent this, system-level design bounds are selected to avoid converter infeasibility from exceeding device ratings, and the parallelization of power converters allows for any power rating to be achieved.

# A. System-Level Optimization

The objectives at the system-level are to minimize required ESS power capacity  $W_{ES}$  and minimize peak grid power  $P_{g(pk)}$ , which relates to the utility infrastructure requirement. These two objectives are inherently conflicting as a larger ESS can allow more smoothing of power from the grid. This results in a Pareto

front showing the trade-off of the two objectives. The design constraints are minimum and maximum bounds on the ESS SOC,  $SOC_{min}$  and  $SOC_{max}$ , and terminal voltage,  $V_{ESS(min)}$  and  $V_{ESS(max)}$ . The design variables for this level should be limited to high-level details that affect the overall performance of the system. Therefore, the design variables are ESS battery pack modules in series  $N_s$ , cells per module  $N_p$ , DC bus voltage  $V_{bus}$ , and the controller time-average window size  $T_w$ . To simplify notation, system design parameters are grouped into a vector  $x_s$ . The system-level problem is formally defined as (7). It is subject to the optimal design parameters of both converter-level problems, represented by the last two rows of (7).

$$\min_{\substack{x_{S},x_{c1},x_{c2}}} \{P_{g(pk)},W_{ES}\}$$

$$s.t. \quad SOC_{min} \leq SOC \leq SOC_{max}$$

$$V_{ESS(min)} \leq V_{ESS} \leq V_{ESS(max)}$$

$$x_{c1} \in \operatorname{argmin}\{eq.(11)\}$$

$$x_{c2} \in \operatorname{argmin}\{eq.(12)\}$$

$$(7)$$

## B. Converter-Level Optimization

For nested bi-level optimization, the lower-level problem can contain either a single or multiple objectives. However, seeking multiple objectives at the converter-level would result in multiple converter design options that the system-level must choose from, requiring further system design evaluations. For this demonstration, the converter design problem is formulated in a way to avoid multiple objectives. Converters are often optimized for an objective of maximum efficiency in practice, where a conflicting objective or limiting constraint would be necessary to avoid simply oversizing the converter. Such conflicting objectives could be to minimize cost or weight. However, weight is of little concern for a stationary power converter. To avoid introducing a cost metric into the design problem, minimizing the number of converters in parallel  $N_{DAB}$ serves as a representative to minimizing cost. As power loss is still a primary concern, a minimum efficiency  $\eta_{min}$  serves as a design constraint. The efficiency constraint considers the maximum output voltage and power, so in application the operating efficiency may be slightly lower.

The remaining constraints are the rated power minimum  $P_{rated(\min)}$  and maximum  $P_{rated(\max)}$ , and the ZVS conditions given in (5)-(6). These constraints are selected to achieve realistic efficiency and proper sizing of the converter. The converter design variables are transformer leakage inductance  $L_t$ , winding turns ratio  $n_t$ , switching frequency  $f_{sw}$ , and the number of converters in parallel  $N_{DAB}$ . Converter design parameters are aggregated into a vector  $\mathbf{x}_{c1}$  for the ESS tied DAB converter, and  $\mathbf{x}_{c2}$  for the charging port DAB converters.

The DAB converters power rating is defined as the maximum possible power output of the converter given an output voltage  $V_0$ , and calculated using (8). The average output current is equivalent to the average inductor current  $I_L$ , found with (9) for positive power flow [13], where  $R = R_t + 2n_t^2 R_{p(on)} + 2R_{s(on)}$ , and  $\theta = R/4f_{sw}L_t$ . The maximum inductor current  $I_{L(max)}$  occurs at the maximum duty

ratio  $d_{max}$ , given in (10).  $d_{max}$  is found by solving for d in  $\partial I_L/\partial d=0$ .

$$P_{rated} = N_{DAB}V_oI_{L(max)} \tag{8}$$

$$I_{L} = \frac{n_{t}V_{in} - V_{o}}{R} + \frac{V_{o}}{\theta R} \tanh(\theta) + \frac{n_{t}V_{in}}{\theta R} \left(1 - 2\theta d - \operatorname{sech}(\theta) e^{\theta - 2\theta d}\right)$$
(9)

$$d_{max} = \frac{\ln(2) - \ln(1 + e^{-2\theta})}{2\theta} \tag{10}$$

For the ESS tied DAB converter, the optimization problem is formally defined as

$$\min_{\substack{x_{c1} \\ x_{c1}}} \{N_{DAB}\}$$

$$s.t. \qquad \eta_{min} \leq \eta_{DAB}$$

$$P_{rated(min)} \leq P_{rated} \leq P_{rated(max)}$$

$$ZVS \ eq. (5)$$

$$ZVS \ eq. (6)$$
(11)

and is dependent on the system-level parameters  $V_{bus}$ ,  $N_s$ , and  $N_p$ . The system-level parameters influence the converters input and output voltages, and the minimum rated power. To ensure the ESS can supply the rated power at all voltage levels, (9) is evaluated using  $V_{in} = V_{ESS(min)}$ . Similarly, the ZVS conditions of (5)-(6) are evaluated at  $P_{rated(min)}$  and  $V_{ESS(min)}$ .

The charging port DAB converters are all sized identically and based on system-level parameter  $V_{bus}$ , HDEV charging voltage minimum  $V_{cp(min)}$  and maximum  $V_{cp(max)}$ , and maximum charging power  $P_{cp(max)}$ . The optimization problem is formally defined as (12). The converter power rating constraint uses  $V_{cp(min)}$  and  $P_{cp(max)}$ .

$$\min_{x_{c2}} \{N_{DAB}\}$$
s.t.  $\eta_{min} \leq \eta_{DAB}$ 

$$P_{rated(min)} \leq P_{rated} \leq P_{rated(max)}$$

$$ZVS \ eq. (5)$$

$$ZVS \ eq. (6)$$
(12)

#### IV. OPTIMIZATION DEMONSTRATION

In this section, the bi-level optimization framework is demonstrated for a HDEVCS with nine charging ports rated for 400 kW each. The charging station simulation is developed in MATLAB/Simulink. System-level optimization uses a multi-objective genetic algorithm (GA) and converter-level optimization is performed using a single-objective GA, both provided in the MATLAB Global Optimization Toolbox. The system-level GA was configured with a population of 75 designs and had a maximum generation count of 150, which equates to approximately 7% of the entire design space. The converter-level GA was configured with a population of 10,000 designs, with a maximum generation count of 500. However, optimization was typically completed with fewer than 200 generations. System-level and converter-level design variable bounds and constraints are listed in Table I. For discussion on

	el and converter-level optimization.

System-level $(x_s)$		Converter-level (ESS DAB) $(x_{c1})$		Converter-level (CP DAB) $(x_{c2})$	
Design Parameter	Range	Design Parameter	Range	Design Parameter	Range
$V_{bus}(V)$	[800:1600]	$L_t(nH)$	[1:1e6]	$L_t(nH)$	[1:1e6]
$T_w$ (hours)	[1:24]	$n_t$ (#)	[0.1:10]	$n_t$ (#)	[0.1:10]
$N_s$ (#)	[200:400]	$f_{sw}(kHz)$	[100:500]	$f_{sw}(kHz)$	[100:500]
$N_p$ (#)	[1000:10,000]	$N_{DAB}$ (#)	[30:80]	$N_{DAB}$ (#)	[5:20]
Constraint Limits		Constraint Limits		Constraint Limits	
$20\% \le SOC \le 95\% \qquad \qquad 95\% \le \eta_{DAB}$		DAB	$95\% \le \eta_{DAB}$		
$3.0 V \le V_{ESS} \le 4.2 V$		$N_p N_s P_{cell} \le P_{rated} \le 1.5 N_p N_s P_{cell}$		$400 \ kW \le P_{rated} \le 600 \ kW$	

how the design variables impact the charging station operation, refer to Section II. The ESS DAB converter  $P_{rated}$  constraint uses the maximum power rating of a battery cell  $P_{cell}$ , approximated as the max C rating current times the nominal voltage.

Each candidate design is evaluated by simulating the charging station for all five Monte Carlo samples (discussed in Section II-B), each of a 24-hour duration. The constraints of (7) are evaluated for all five simulations, while the maximum  $P_{g(pk)}$  is used as the objective. An example charging load and the power delivered by the ESS and grid, along with the ESS SOC, is shown in Fig. 5. In this case, a 12-hour  $T_w$  is used, yielding a peak grid power of 2 MW.

The resulting Pareto front for the two objectives, minimum  $W_{ES}$  and  $P_{g(pk)}$  is shown in Fig. 6, where the expected trend of increasing  $W_{ES}$  causing a corresponding decrease in  $P_{g(pk)}$  is observed. The bias constant  $P_{bias}$  of the grid power controller causes the absolute minimum  $P_{g(pk)}$  to be 1 MW (assuming no power losses and the average number of EV arrivals), where the ESS would mitigate all load changes. Aside from this minimum, any peak grid power can be achieved with sufficient  $W_{ES}$ . However, reducing the peak grid power to  $P_{bias}$  will require a very large ESS investment due to the nonlinear relation between  $W_{ES}$  and  $P_{g(pk)}$ . In other words, to reduce  $P_{g(pk)}$  by 0.5 MW near its lower limit requires two times as much  $W_{ES}$ . While all designs on the Pareto front are technically optimal solutions, the

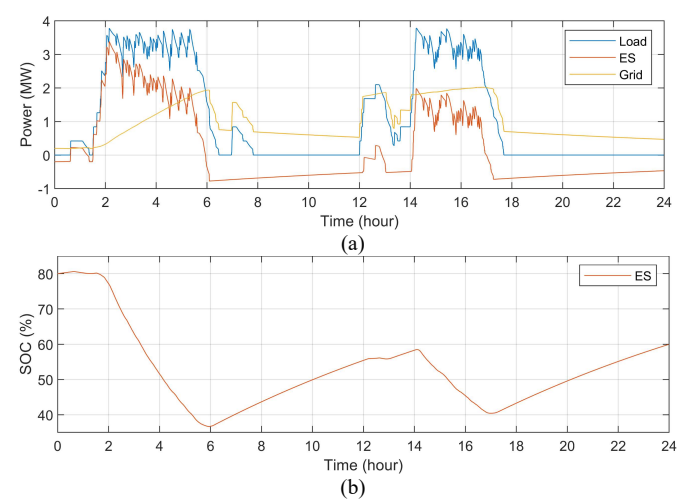


Fig. 5. Charging station power demand, (a) ES/grid load distribution, and (b) ES SOC for a 24-hour simulation.

achieved reduction in  $P_{g(pk)}$  clearly diminishes with an ESS size greater than 15 MWh. This design scenario suggests that additional ESS capacity beyond 15 MWh would not be economical.

Fig. 6 also includes the alternative Pareto fronts if the converter power losses were modeled with fixed efficiency values, which were used mostly in other literature but are replaced by actual efficiency numbers in this paper. Since efficiency numbers vary between sources found in the literature, three fixed efficiencies will be compared to the bi-level framework. Instead of running a new optimization procedure for each approach, the Pareto optimal designs found from the bilevel framework are simulated again under the same charging station load conditions, this time with fixed efficiency. This method of comparison is chosen instead of performing a whole new optimization procedure to ensure the variations in the Pareto front are clear. If a whole new optimization procedure was executed for each fixed efficiency station model, there would be no guarantee that each Pareto front would be comparable due to the randomness within the GA and the absence of ESS voltage constraints.

The new Pareto fronts using  $\eta = 95\%$ ,  $\eta = 97\%$ , and  $\eta = 100\%$  converter efficiencies are shown in Fig. 6. To avoid altering the power management controls,  $W_{ES}$  for the fixed efficiency charging station simulations are configured the same as the bi-level simulation. The alternative ESS sizes shown in

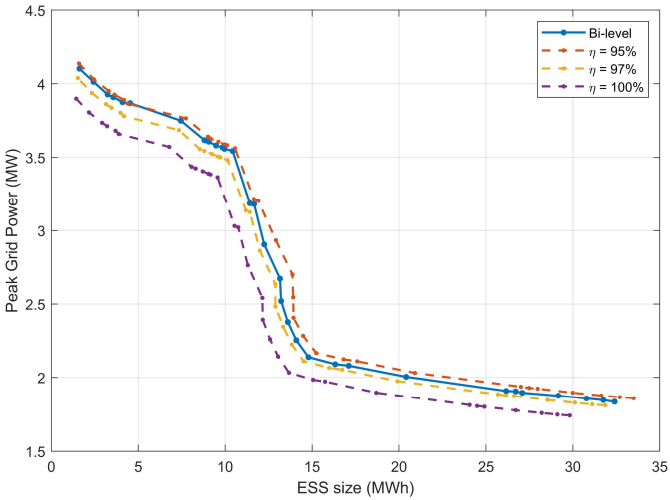


Fig. 6. System-level Pareto fronts for the bi-level framework that uses power loss models, and an ideal charging station model.

Fig. 6 represent the equivalent ESS size, provided each approach had an equivalent ESS depth of discharge. In other words, the alternative ESS sizes in Fig. 6 are the required energy capacity using an ideal ESS and fixed efficiency power electronic converters.

For all Pareto optimal designs,  $\eta=97\%$  and  $\eta=100\%$  result in an underestimate of the required  $W_{ES}$ , while  $\eta=95\%$  results in an overestimate. Similarly,  $P_{g(pk)}$  are universally lower than the  $P_{g(pk)}$  values for  $\eta=97\%$  and  $\eta=100\%$  compared to the bi-level approach. From Fig. 6, it can also be concluded that the changes in objective values between the bi-level and fixed efficiency approaches cannot simply be represented by linear scaling, as the deviation from the bi-level Pareto front is not constant. This can be attributed to the power loss models used in the bi-level approach that result in nonconstant efficiencies. This comparison to charging station simulations using fixed efficiency components demonstrates the improvements in optimization and sizing accuracy provided by the bi-level framework.

#### V. CONCLUSION AND FUTURE WORK

To independently supply the high peak power demand of HDEVCS, grid infrastructure may be subject to much higher loads, greatly increasing the investment cost. This peak power can be mitigated through on-site ESS that offsets the energy during peak hours. Considering the trade-off between ESS size and the peak power experienced by the grid is key to charging station design. To analyze this trade-off, Pareto optimal designs are found using a bi-level optimization framework that considers the design and impact of power electronic converters within the station. The bi-level hierarchy separates the problem of ESS size and peak power minimization from the problem of converter design. By incorporating converter design and power loss models within the sizing problem can lead to more informed design decisions.

Future work to improve the optimization approach includes increasing the number of Monte Carlo simulations, or finding an alternative, approximate approach to capturing the variability in charging station loads. Converter design can be enhanced by including thermal management constraints. A battery lifetime constraint can also be added to the system level design problem, ensuring the ESS lasts for the desired amount of time.

#### ACKNOWLEDGEMENT

This work was supported in part by Portland General Electric and in part by the U.S. National Science Foundation (NSF) Award ECCS-2146350.

#### REFERENCES

- [1] X. Zhu, R. Mahmud, B. Mather, P. Mishra and A. Meintz, "Grid Voltage Control Analysis for Heavy-Duty Electric Vehicle Charging Stations," in Proc. IEEE PES Innovative Smart Grid Technologies Conference (ISGT), 2021, pp. 1-5.
- [2] T. Li et al., "An Optimal Design and Analysis of a Hybrid Power Charging Station for Electric Vehicles Considering Uncertainties," in *Proc. IEEE Industrial Electronics Society Conf. (IECON)*, 2018, pp. 5147-5152.
- [3] A. Hussain, V. Bui and H. Kim, "Optimal Sizing of Battery Energy Storage System in a Fast EV Charging Station Considering Power Outages," in *IEEE Transactions on Transportation Electrification*, vol. 6, no. 2, pp. 453-463, 2020.

- [4] S. N. Hashemian, M. A. Latify and G. R. Yousefi, "PEV Fast-Charging Station Sizing and Placement in Coupled Transportation-Distribution Networks Considering Power Line Conditioning Capability," in *IEEE Transactions on Smart Grid*, vol. 11, no. 6, pp. 4773-4783, 2020.
- [5] Rehman, Waqas Ur & Bo, Rui & Mehdipourpicha, Hossein & Kimball, J.W., "Sizing Energy Storage System for Energy Arbitrage in Extreme Fast Charging Station," in *Proc. IEEE PES General Meeting*, 2021, pp. 1-6.
- [6] Hussain, Akhtar, Van-Hai Bui, Ju-Won Baek, and Hak-Man Kim, "Stationary Energy Storage System for Fast EV Charging Stations: Simultaneous Sizing of Battery and Converter," in *Energies*, vol. 12, no. 23, pp. 1-17, 2019.
- [7] G. Liu, M. S. Chinthavali, S. Debnath and K. Tomsovic, "Optimal Sizing of an Electric Vehicle Charging Station with Integration of PV and Energy Storage," in *Proc. IEEE Power & Energy Society Innovative Smart Grid Technologies Conference (ISGT)*, 2021, pp. 1-5.
- [8] A. Sinha, P. Malo and K. Deb, "A Review on Bilevel Optimization: From Classical to Evolutionary Approaches and Applications," in *IEEE Transactions on Evolutionary Computation*, vol. 22, no. 2, pp. 276-295, 2018.
- [9] Y. Cao, R. C. Kroeze, and P. T. Krein, "Multi-timescale Parametric Electrical Battery Model for Use in Dynamic Electric Vehicle Simulations," in *IEEE Trans. Transportation Electrification*, vol. 2, no. 4, pp. 432-442, 2016
- [10] H. Tu, H. Feng, S. Srdic and S. Lukic, "Extreme Fast Charging of Electric Vehicles: A Technology Overview," in *IEEE Transactions on Transportation Electrification*, vol. 5, no. 4, pp. 861-878, 2019.
- [11] M. Ahmadi, N. Mithulananthan and R. Sharma, "A review on topologies for fast charging stations for electric vehicles," in *Proc. IEEE International Conference on Power System Technology (POWERCON)*, 2016, pp. 1-6.
- [12] F. Zhang, M. M. U. Rehman, R. Zane and D. Maksimović, "Improved steady-state model of the dual-active-bridge converter," in *Proc. IEEE Energy Conversion Congress and Exposition (ECCE)*, 2015, pp. 630-636.
- [13] J. A. Mueller and J. W. Kimball, "An Improved Generalized Average Model of DC–DC Dual Active Bridge Converters," in *IEEE Transactions on Power Electronics*, vol. 33, no. 11, pp. 9975-9988, 2018.
- [14] K. George, "Design and Control of a Bidirectional Dual Active Bridge DC-DC Converter to Interface Solar, Battery Storage, and Grid-Tied Inverters," Electrical Engineering Undergraduate Honors Thesis, University of Arkansas, 2015.